JOURNAL OF AIRCRAFT
Vol. 46, No. 5, September–October 2009

Numerical Evaluation of Limit Cycles of Aeroelastic Systems

Mauro Manetti,* Giuseppe Quaranta,† and Paolo Mantegazza‡
Politecnico di Milano, 20156 Milan, Italy

DOI: 10.2514/1.42928

This paper focuses on the analysis of limit-cycle oscillations of aeroelastic systems with multiple lumped nonlinearities. It aims at a comprehensive investigation capable of identifying limit cycles and their stability. The goal is achieved by using an incremental complexity approach. At the beginning, a solution based on dual-input describing functions is sought, to find both symmetric and asymmetric cycles approximated to their first harmonic. The related stability is investigated afterward by extending the single-input describing function "quasi-static" method. Such an approach is simple and quite similar to well-established existing methods used to evaluate linear flutter conditions directly. If higher harmonics are required, an extended harmonic balance based on a numerical minimization in the frequency domain is adopted and the stability of the computed solutions is then determined by using Floquet theory. The presented approach is applied to several nonlinear aeroelastic examples and validated by comparing stable limit cycles with solutions obtained through direct time marching integrations.

Nomenclature

$\boldsymbol{A}_a, \boldsymbol{B}_a, \boldsymbol{C}_a$	=	aerodynamics state-space matrices
$\boldsymbol{a}$	=	aerodynamic state vector
$\arg(\cdot)$	=	phase of a complex number, $\tan^{-1}(\Im/\Re)$
$\bar{\boldsymbol{B}}_{\text{nl}}$	=	input matrix for lumped nonlinearities on structural degrees of freedom
$\boldsymbol{b}_i$	=	real Fourier coefficients
$\boldsymbol{C}$	=	structural damping matrix
$\boldsymbol{c}_i$	=	imaginary Fourier coefficient
$\boldsymbol{D}_0, \boldsymbol{D}_1, \boldsymbol{D}_2$	=	aerodynamics quasi-steady matrices
$\det(\cdot)$	=	matrix determinant
$\text{diag}(\cdot)$	=	diagonal matrix
$\boldsymbol{F}_a$	=	generalized aerodynamic forces, Nm
G	=	transfer function
H_n	=	Fourier coefficient $\in \mathbb{C}$
h	=	plunge displacement
$\boldsymbol{I}$	=	unit matrix
$\Im[\cdot]$	=	imaginary part of a complex number
J	=	moment of inertia, kgm^2
j	=	imaginary unit
$\boldsymbol{K}$	=	structural stiffness matrix
l_a	=	reference length, m
$\boldsymbol{M}$	=	structural mass matrix
M_∞	=	Mach number
m	=	mass, kg
N	=	describing function coefficients $\in \mathbb{C}$
$\boldsymbol{Q}$	=	transition matrix
$\boldsymbol{q}$	=	generalized structural degrees of freedom
q_∞	=	dynamic pressure, Pa
$\Re[\cdot]$	=	real part of a complex number
r	=	radius of gyration
S	=	first mass moment, kgm
s	=	complex variable
T	=	period, s
$\boldsymbol{u}$	=	structural nodes displacement vector
V_∞	=	reference velocity, m/s
$\boldsymbol{x}$	=	spatial coordinates
$\boldsymbol{z}$	=	global state vector
α	=	pitch rotation, rad
α_{lc}	=	limit-cycle scalar amplitude
β_i	=	displacement of the ith lumped nonlinearity
$\dot{\beta}_i$	=	velocity of the ith lumped nonlinearity
$\boldsymbol{\gamma}$	=	describing function bias vector
$\boldsymbol{\delta}$	=	describing function amplitude vector
$\boldsymbol{\varepsilon}$	=	residual vector
η_i	=	complex Fourier coefficients
μ	=	mass ratio
ρ	=	air density, kg/m^3
ζ_i	=	real Fourier coefficients
$\boldsymbol{\Phi}$	=	structural shape functions
ω	=	circular frequency, rad/s

Subscripts

d	=	dual input
h	=	plunge
lc	=	limit cycle
nl	=	nonlinear
ql	=	quasi linearized
α	=	pitch
β	=	flap

I. Introduction

ROUTINE flutter analyses are carried out mostly on linearized models, both for the structure and the aerodynamics. They provide results that are often in good agreement with test outcomes. Nonetheless, the assumption of negligible nonlinearities may sometimes hide problems revealed only during test and certification phases.

In general, nonlinearities in the fluid and/or the structure result in complex system behaviors, such as limit-cycle oscillations (LCOs), that are of much interest in aircraft design, because system stability may become dependent on the amplitude of the disturbance. Using a nonlinear dynamics point of view, the crossing of the flutter onset leads to a Hopf bifurcation where a periodic self-sustained motion, the LCO, branches from a given equilibrium solution [1]. The frequency and amplitude characteristics of the LCO depend on the dynamic system properties only.

The first studies on structural lumped nonlinearities in aeroelasticity began in the 1950s [2,3]. Nonlinearities were used to represent free play of mechanisms, friction in bearings, cables, bars, and servo-actuator systems. Aerodynamic nonlinearities may also

Received 25 December 2008; revision received 14 May 2009; accepted for publication 18 May 2009.

*Ph.D. Candidate, Dipartimento di Ingegneria Aerospaziale, Via La Masa, 34; manetti@aero.polimi.it.

†Postdoctoral Research Fellow, Dipartimento di Ingegneria Aerospaziale, Via La Masa, 34; giuseppe.quaranta@polimi.it.

‡Full Professor, Dipartimento di Ingegneria Aerospaziale, Via La Masa, 34; paolo.mantegazza@polimi.it.

lead to LCOs, as shown, for example, in [4]. A review of the basic nonlinear aeroelastic phenomena can be found in [5–7].

To investigate quantitatively the asymptotic behavior of a nonlinear system, it is possible to compute the response by using a direct time marching numerical integration for a sufficiently long time window. This approach is straightforward but, when multiple solutions are possible, the computed periodic movement is highly sensitive to initial conditions. Therefore, time marching techniques are of limited value, unless an extensive survey of possible initial conditions is conducted. In any case, such an approach is computationally expensive, especially in conceptual and preliminary, possibly up to intermediate, design phases, when there is the need to assess possible LCO effects on the system without verifying any response in detail. A more efficient approach can be built by exploiting the fact that the asymptotic solution is periodic in time. In this case, the LCO can be expressed by using a Fourier series in time resulting in different approximation levels, depending on the number of harmonics retained; to understand if the asymptotic solution is feasible, it is necessary to investigate its stability properties. Under this class fall the well-known methods denominated harmonic balance or describing function (DF) [8], often used mainly to point out cases where only the fundamental harmonic is adequate to describe the LCO. This approach has been successfully employed in many aeroelastic applications [9–13]. A detailed comparison of results obtained by using different numerical methods is shown in [14]. The procedure is straightforward but requires the computation of integrals to assemble the set of nonlinear algebraic equations needed to solve for the Fourier coefficients, which are particularly cumbersome when a high number of harmonics are required [15].

Stemming from [16,17], we propose here an incremental complexity approach to overcome this problem. At first, a quasi linearization of the aeroelastic systems with multiple concentrated nonlinearities is developed by using dual-input describing functions (DIDFs) [8,9,18,19] to handle both symmetric and nonsymmetric LCOs. The related problem is then cast into a nonlinear system of equations, which is effectively solved by extending the use of well-established methods already available for the direct calculation of linear flutter points and sensitivities [20–23] to easily handle large sets of parametrized aeroelastic analyses. The stability of the obtained LCOs is investigated by exploiting and extending the concept of quasi-static stability [8] in a way that is self-contained in the adopted solution technique. The first harmonic solution obtained is often adequate to represent the LCO, because the structure and the aerodynamics act as a low-pass filter with respect to high-frequency oscillations. Nonetheless, in some cases, there is the need of more accurate solutions taking into account higher harmonics.

To avoid the need to compute complex analytical expressions, the problem can be cast in the time domain, similar to what is done in the time domain harmonic balance approach [15]. To such an aim, a high-fidelity periodic solution based on any number of harmonics can be obtained by implementing a functional minimization in the frequency domain finalizing the work presented in [16,17,24,25]. This allows complex types of nonlinearities improving the solution accuracy with higher harmonic contributions to be easily handled. The minimization can be profitably started on the base of an LCO approximation obtained through DIDFs. The stability of such improved solutions can then be inferred by using classical Floquet theory. It must be remarked that the application to aeroelastic problems does not limit the generality of the methods presented here, which can be employed to study any generic autonomous systems with lumped nonlinearities.

The paper is organized as follows. Section II recalls the dual-input DF, whereas Sec. III shows how to find LCO characteristics by solving a nonlinear system of equations. Section IV presents the extension to higher harmonics, whereas Sec. V is dedicated to the stability investigation. Finally, Sec. VI presents the study of several aeroelastic models related to typical sections [26] with 2 and 3 degrees of freedom (DOF) in subsonic unsteady flow and a 5 DOF tail in supersonic regime. The used nonlinearities include hysteresis, asymmetry, and discontinuity, as well as multiple lumped nonlinearities.

II. Dual-Input Describing Functions

The DF is based on the application of quasi linearization, that is, the approximation of the nonlinear system under investigation by a sort of linear model, where a dependence is left on the amplitude of the input [8,18]. A quasi-linearized system is more difficult to handle than a linear one, nonetheless, it retains the possibility of sharing some analysis methods typical of those systems. The quasi linearization is apt to reproduce the overall nonlinear response if the linear part of the system acts as a low-pass filter with a passband low enough to rule higher harmonics out of the response. This low-pass filtering hypothesis is usually verified but it is rarely possible to check it up front, and so the DF method is often considered an empiric approach.

Let us consider a sinusoidal signal plus a bias defined by the real numbers (γ, δ, ω)

$$x_{\mathrm{nl}}(t) = \gamma + \delta\cos(\omega t) \tag{1}$$

as the input of a nonlinear element. The corresponding output is equal to

$$y_{\mathrm{nl}}(t) = f[\gamma + \delta\cos(\omega t)] \tag{2}$$

The output can be expressed by using a Fourier series

$$y_{\mathrm{nl}}(t) = \sum_{n=0}^{\infty} |H_n(\omega, \gamma, \delta)|\cos\{n\omega t + \arg[H_n(\omega, \gamma, \delta)]\} \tag{3}$$

where $H_n \in \mathbb{C}$ are the Fourier coefficients. Such coefficients are functions of input bias and amplitude because they describe the output of a nonlinear element. Using only the first harmonic plus the bias term, the DIDF is obtained

$$y_d(t) = N_\gamma\gamma + \{\Re[N_\delta]\cos(\omega t) + \Im[N_\delta]\sin(\omega t)\}\delta \tag{4}$$

where

$$N_\gamma(\omega, \delta, \gamma) = \frac{H_0}{\gamma} \qquad \in \mathbb{R} \tag{5}$$

$$N_\delta(\omega, \delta, \gamma) = \frac{\| H_1 \|}{\delta} e^{j\arg(H_1)} \qquad \in \mathbb{C} \tag{6}$$

In general, it is possible to build several types of describing functions with different approximation levels, depending on the number of Fourier terms kept. Nonetheless, the preceding dual-input class is often good enough to obtain solutions efficiently when a large set of parametrized analyses is required.

Consider a lumped nonlinear element in feedback to a linear system, characterized by its frequency response function $G(j\omega)$, as shown in Fig. 1. The output of the linear block for the quasi-linearized system is equal to

$$\begin{aligned} y(t) = Gx(t) = -Gy_{\mathrm{nl}}(t) \simeq -Gy_d(t) = -G(j0)N_\gamma\gamma \\ + -(\Re[N_\delta]\{\Re[G(j\omega)]\sin(\omega t) + \Im[G(j\omega)]\cos(\omega t)\} \\ + -\Im[N_\delta]\{\Re[G(j\omega)]\cos(\omega t) + \Im[G(j\omega)]\sin(\omega t)\})\delta \end{aligned} \tag{7}$$

At the limit-cycle condition $y = x_{\mathrm{nl}}$, so that by Eqs. (1) and (7)

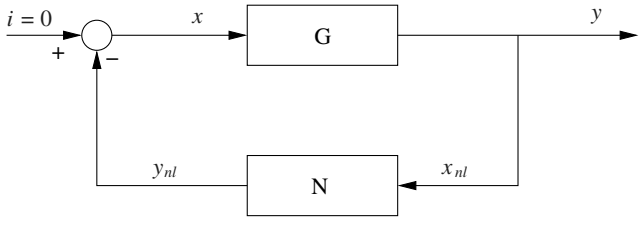

Fig. 1 Quasi-linearized system representation in the feedback equivalent form.

$$-G(j0)N_\gamma(\omega,\delta,\gamma)\gamma=\gamma \tag{8}$$

$$-G(j\omega)N_\delta(\omega,\delta,\gamma)\delta=\delta \tag{9}$$

It should be noticed that a null right-hand side term is often used in place of γ in Eq. (8) [18,27]; the reader should refer to [8] for an explanation of such a simplification. Equations (8) and (9) are coupled scalar and complex equations, respectively. The solution of the corresponding set of three real nonlinear algebraic equations is used to compute the unknown parameters characterizing the limit-cycle response, that is, δ, γ, and ω. If the system under investigation does not present a nonsymmetric nonlinearity, the bias γ disappears and Eq. (9) is the only one to be verified. Thus, the DIDF is a generalization of the single-input method useful to find LCO conditions for symmetric/nonsymmetric nonlinearities.

III. Limit-Cycle Oscillation for Multiple Nonlinearities with Describing Function

The application of the approach presented in the previous section to multi-degrees-of-freedom systems with multiple lumped nonlinearities requires further developments. Therefore, to correctly recover the first harmonic component and any possible bias vector of a limit cycle using DIDFs, the procedure is appropriately reworked. Moreover, to enable a broader treatment and an easier implementation in a general purpose aeroelastic analysis, all dynamic systems are set in a state-space form. To this end, the linear model of the structural system can be written as

$$\boldsymbol{M}\ddot{\boldsymbol{q}}+\boldsymbol{C}\dot{\boldsymbol{q}}+\boldsymbol{K}\boldsymbol{q}=\boldsymbol{F}_a \tag{10}$$

where $\boldsymbol{q}$ is an appropriate set of free generalized structural degrees of freedom associated with the shape functions $\boldsymbol{\Phi}(\boldsymbol{x})$ which describe the displacement field $\boldsymbol{u}(\boldsymbol{x})$ through a Ritz discretization

$$\boldsymbol{u}(\boldsymbol{x},t)=\boldsymbol{\Phi}(\boldsymbol{x})\boldsymbol{q}(t) \tag{11}$$

$\boldsymbol{x}$ being the space coordinates. Also, the unsteady generalized aerodynamic forces associated with the structural degrees of freedom can be transformed from classical frequency domain expressions into a state-space system, using finite state approximations (see, for example, [28] and references thereof),

$$\left(\frac{l_a}{V_\infty}\right)\dot{\boldsymbol{a}}=\boldsymbol{A}_a\boldsymbol{a}+\boldsymbol{B}_a\boldsymbol{q}$$

$$\boldsymbol{F}_a=q_\infty\left[\boldsymbol{C}_a\boldsymbol{a}+\boldsymbol{D}_0\boldsymbol{q}+\left(\frac{l_a}{V_\infty}\right)\boldsymbol{D}_1\dot{\boldsymbol{q}}+\left(\frac{l_a}{V_\infty}\right)^2\boldsymbol{D}_2\ddot{\boldsymbol{q}}\right] \tag{12}$$

with q_∞ used to indicate the dynamic pressure. As a result, the following nonlinear time-invariant aeroelastic system in descriptor form is obtained:

$$\boldsymbol{E}\dot{\boldsymbol{z}}=\boldsymbol{A}\boldsymbol{z}+\boldsymbol{B}_{\rm nl}\boldsymbol{f}_{\rm nl} \tag{13}$$

The state vector is composed by $\boldsymbol{z}^T=[\,\boldsymbol{q}^T\quad\dot{\boldsymbol{q}}^T\quad\boldsymbol{a}^T\,]$, and so the state matrices are equal to

$$\boldsymbol{E}=\begin{bmatrix}\boldsymbol{I}&0&0\\0&\left[\boldsymbol{M}-q_\infty\left(\frac{l_a}{V_\infty}\right)^2\boldsymbol{D}_2\right]&0\\0&0&\boldsymbol{I}\end{bmatrix}$$

$$\boldsymbol{A}=\begin{bmatrix}0&\boldsymbol{I}&0\\-(\boldsymbol{K}-q_\infty\boldsymbol{D}_0)&-\left[\boldsymbol{C}-q_\infty\left(\frac{l_a}{V_\infty}\right)\boldsymbol{D}_1\right]&q_\infty\boldsymbol{C}_a\\0&\frac{V_\infty}{l_a}\boldsymbol{B}_a&\frac{V_\infty}{l_a}\boldsymbol{A}_a\end{bmatrix}$$

$\boldsymbol{B}_{\rm nl}^T=[\,\boldsymbol{0}^T\quad\tilde{\boldsymbol{B}}_{\rm nl}^T\quad\boldsymbol{0}^T\,]$ is the input matrix for the multiple lumped nonlinearities joined in the vector $\boldsymbol{f}_{\rm nl}$. The ith component $f_{{\rm nl}_i}=f(\beta_i,\dot{\beta}_i)$ is function of the displacement and velocity of the ith nonlinear degree of freedom. These physical degrees of freedom β_i are recovered from the structural generalized coordinate $\boldsymbol{q}$ by appropriate connection relations that can be expressed as

$$\beta_i=\boldsymbol{\Psi}_i\boldsymbol{q}\quad\text{and}\quad\dot{\beta}_i=\boldsymbol{\Psi}_i\dot{\boldsymbol{q}} \tag{14}$$

$\boldsymbol{\Psi}_i$ being a connection matrix.

In LCO conditions, it is possible to use DIDFs to approximate the nonlinear output representing it through two contributions:

$$f_{{\rm nl}_i}(\beta_i,\dot{\beta}_i)\simeq f_{d1}(N_{i\gamma},\beta_i)+f_{d2}(N_{i\delta},\beta_i,\dot{\beta}_i) \tag{15}$$

To obtain a linear system, the bias contribution f_{d1} has to be temporarily removed. Such a contribution will be recovered later on, in a consistent way, by adding an appropriate equation for each nonlinearity. The term $N_{i\delta}(\delta_i,\gamma_i)$ is a complex function; by transforming it into the time domain and using the relation between the physical degrees of freedom β_i and the generalized coordinates, the following relation results:

$$f_{d2}=\Re[N_{i\delta}]\boldsymbol{\delta}+\Im[N_{i\delta}]\dot{\boldsymbol{\delta}}\equiv\Re[N_{i\delta}]\boldsymbol{\Psi}_i\boldsymbol{q}+\Im[N_{i\delta}]\boldsymbol{\Psi}_i\dot{\boldsymbol{q}} \tag{16}$$

Premultiplying by the corresponding column of the matrix $\tilde{\boldsymbol{B}}_{\rm nl}^T$, additional stiffness $\tilde{\boldsymbol{K}}_i$ and damping $\tilde{\boldsymbol{C}}_i$ matrices are obtained for each nonlinear function. A consistent application of such a quasi linearization to all nonlinear terms leads to a new autonomous system

$$\boldsymbol{E}\,\dot{\boldsymbol{z}}=\boldsymbol{A}_{\rm ql}\boldsymbol{z} \tag{17}$$

where the quasi-linearized state matrix $\boldsymbol{A}_{\rm ql}$ maintains the same structure as the already-seen matrix $\boldsymbol{A}$, but with the structural stiffness and damping $\boldsymbol{K}$ and $\boldsymbol{C}$ matrices replaced by

$$\boldsymbol{K}_e=\boldsymbol{K}+\sum_i\tilde{\boldsymbol{K}}_i \tag{18}$$

$$\boldsymbol{C}_e=\boldsymbol{C}+\sum_i\tilde{\boldsymbol{C}}_i \tag{19}$$

For any feasible LCO condition, the following problem must have a solution $\boldsymbol{Z}_{\rm lc}$ different from the trivial null one

$$[-j\omega_{\rm lc}\boldsymbol{E}+\boldsymbol{A}_{\rm ql}(\omega_{\rm lc},\boldsymbol{\gamma},\boldsymbol{\delta})]\boldsymbol{Z}_{\rm lc}=\boldsymbol{0} \tag{20}$$

The unknowns are as follows: the limit-cycle circular frequency $\omega_{\rm lc}$, the bias and first harmonic amplitude vectors $\boldsymbol{\gamma}$ and $\boldsymbol{\delta}$, and the vector $\boldsymbol{Z}_{\rm lc}\in\mathbb{C}$. The amplitude vector $\boldsymbol{\delta}$ and its time derivative $\dot{\boldsymbol{\delta}}$ are linearly dependent on the structural degrees of freedom $\boldsymbol{q}$ and $\dot{\boldsymbol{q}}$ as shown by Eq. (14). Therefore, it is correct to express Eq. (20) as

$$[-j\omega_{\rm lc}\boldsymbol{E}+\boldsymbol{A}_{\rm ql}(\omega_{\rm lc},\boldsymbol{Z}_{\rm lc},\boldsymbol{\gamma})]\boldsymbol{Z}_{\rm lc}=\boldsymbol{0} \tag{21}$$

Equation (21) is a homogeneous system that looks like an eigenvalue problem in $\omega_{\rm lc}$ and $\boldsymbol{\gamma}$. However, not all of the amplitudes of vector $\boldsymbol{Z}_{\rm lc}$ are valid, but only those that solve the equation

$$\det[-j\omega_{\rm lc}\boldsymbol{E}+\boldsymbol{A}_{\rm ql}(\omega_{\rm lc},\boldsymbol{Z}_{\rm lc},\boldsymbol{\gamma})]=0 \tag{22}$$

Equation (22) is complex, and so needs two real unknowns. One of them is clearly $\omega_{\rm lc}$, whereas the other is somewhat hidden in $\boldsymbol{Z}_{\rm lc}$, its amplitude being the missing piece. There can be many ways to point out explicitly such an unknown; here, we choose to add a normalization condition on the vector $\boldsymbol{Z}_{\rm lc}$ through a scaling factor $\alpha_{\rm lc}$, that is,

$$\boldsymbol{Z}_{\rm lc}=\alpha_{\rm lc}\boldsymbol{Z}_u,\qquad\boldsymbol{Z}_u^T\boldsymbol{Z}_u=1 \tag{23}$$

Equation (20) is the generalization of Eq. (9) to a problem with multiple lumped nonlinearities. The difference is due to the dependence of the limit-cycle amplitude $\boldsymbol{\delta}$ from the eigenvector $\boldsymbol{Z}_{\rm lc}$ itself. To account for a possible bias, it is necessary to add the equivalent of Eq. (8). In this case, the static gain $G_i(j0)$ of the ith nonlinear element can be easily computed, and so, for each term of the bias vector, an equation of the type

$$G_i(j0)N_{i\gamma}(\omega_{\rm lc}, \boldsymbol{Z}_u, \alpha_{\rm lc}, \gamma_i)\gamma_i + \gamma_i = 0 \tag{24}$$

can be written. Summarizing, the LCO is found by solving the following nonlinear system of complex equations:

$$\begin{cases} [-j\omega_{\rm lc}\boldsymbol{E} + \boldsymbol{A}_{\rm ql}(\omega_{\rm lc}, \boldsymbol{Z}_u, \alpha_{\rm lc}, \boldsymbol{\gamma})]\boldsymbol{Z}_{\rm lc} = \boldsymbol{0} \\ \boldsymbol{Z}_u^T\boldsymbol{Z}_u = 1 \\ \text{diag}[G_i(j0)N_{i\gamma}(\omega_{\rm lc}, \boldsymbol{Z}_u, \alpha_{\rm lc}, \boldsymbol{\gamma})]\boldsymbol{\gamma} + \boldsymbol{\gamma} = \boldsymbol{0} \end{cases} \tag{25}$$

Apart from the bias equations, one should note the striking similarity of the preceding equation with the direct calculation of the linear flutter condition presented in [21], with $\alpha_{\rm lc}$ which plays the role of the flutter dynamic pressure. In fact, a limit cycle is a finite amplitude flutter continuously spread over subdomains of the flight envelope in the plane $q_\infty - M_\infty$.

If the problem has m lumped nonlinearities and n states, the unknowns budget is as follows: n complex unknowns for the vector $\boldsymbol{Z}_u$, which can be decomposed into its real and imaginary parts for a total of $2n$ variables, and m scalar bias terms γ_i and the two scalar variables $\omega_{\rm lc}$ and $\alpha_{\rm lc}$. System (25) is composed of $n+1$ complex equations and m real equations, resulting in $2n+2+m$ real equations. The solution of Eq. (25) can be obtained by using the classical Newton–Raphson method. The choice of the starting point for the iterative algorithm is essential to ensure the convergence to a solution. A good approach is to assign an initial value to $\alpha_{\rm lc}$ belonging to a range for which the resulting initial quasi-linear stiffness $\bar{\boldsymbol{K}}_i$ and damping $\bar{\boldsymbol{C}}_i$ are meaningful in a physical sense, whereas the initial modal shape $\boldsymbol{Z}_{\rm lc}$ has to be close to the expected limit cycle. In this way, it is possible to check even the presence of multiple limit-cycle solutions.

In practice, there is always the need to evaluate the evolution of the system solutions parametrized on design variables and/or different operating conditions. For this reason, we propose here the adoption of a continuation approach [20,29]. This method implies the differentiation of Eq. (25) with respect to a reference parameter of interest p (e.g., V_∞, q_∞, M_∞, or any design parameter) thus obtaining a system of ordinary differential equations. The differentiation of the system with respect to p can be written as

$$\begin{cases} \dfrac{\rm d}{{\rm d}p}\{[-j\omega_{\rm lc}\boldsymbol{E} + \boldsymbol{A}_{\rm ql}(\omega_{\rm lc}, \boldsymbol{Z}_u, \alpha_{\rm lc}, \boldsymbol{\gamma})]\boldsymbol{Z}_{\rm lc}\} = \boldsymbol{0} \\ \dfrac{\rm d}{{\rm d}p}(\boldsymbol{Z}_u^T\boldsymbol{Z}_u - 1) = 0 \\ \dfrac{\rm d}{{\rm d}p}\{\text{diag}[G_i(j0)N_{i\gamma}(\omega_{\rm lc}, \boldsymbol{Z}_u, \alpha_{\rm lc}, \boldsymbol{\gamma})]\boldsymbol{\gamma} + \boldsymbol{\gamma}\} = \boldsymbol{0} \end{cases} \tag{26}$$

Then, Eq. (25) becomes a system of nonlinear differential equations which can be solved by integrating with respect to the variable p. To be well posed, Eq. (26) requires appropriate initial conditions, that is, the limit-cycle solution at the starting parameter p_0. These initial conditions can be computed by solving Eq. (25) through the Newton–Raphson approach. Once the starting solution has been obtained, it is possible to use whatever numerical technique to solve the nonlinear differential problem. An efficient method, which avoids the drifting of a pure differential continuation, is the so-called predictor-algebraic corrector [20,22]: a differential equations solver is used as a predictor to obtain an initial solution at the incremented parameter value, then a Newton–Raphson method, or any of its modifications, is applied to solve the original nonlinear complex algebraic system. Usually, a variable step differential equation solver is used, so that when the algebraic corrector does not converge to the searched solution within an assigned number of steps, it is possible to restart the predictor using a smaller integration step. In this way, the initial solution provided to the algebraic corrector is expected to be closer to its domain of attraction. Similar to what is found in parametrized linear flutter analyses [22], if such a procedure fails to converge, it is because there is either no limit cycle anymore or a new one with different modal participation has to be established by setting a new initial condition. The implementation presented in this work uses a simple forward Euler predictor for Eq. (26), whereas the corrector is the iterative solution of Eq. (25) through Newton–Raphson. It should be noted that the Jacobian matrix remains the same for both the differential predictor and algebraic corrector.

We finally note that, in view of the purely harmonic approximation entailed by multiple DIDFs, it would be possible to cast the whole procedure described earlier by using the classical flutter analysis framework in the frequency domain:

$$[j\omega_{\rm lc}^2\boldsymbol{M} + j\omega_{\rm lc}\boldsymbol{C} + \boldsymbol{K} - q_\infty\boldsymbol{H}_{\rm am}(\omega_{\rm lc}l_a/V_\infty, M_\infty)]\boldsymbol{q} = \boldsymbol{f}_{\rm nl} \tag{27}$$

in place of Eq. (13). Here, $\boldsymbol{H}_{\rm am}$ is the aerodynamic transfer matrix related to structural harmonic motions, which is often at the base of the identification procedure leading to Eq. (12). Such an approach would have the advantage of almost halving the number of unknowns of the nonlinear systems of equations to be solved. That is true indeed; Cardani and Mantegazza [20] use such an approach, but Eq. (27) is unsuitable for the following extension to higher order harmonic approximations, as well as for numerical verifications by time integration, whereas Eq. (13) unifies any type of analysis used in this work. Moreover, because nowadays aeroelasticians are no more involved in aeromechanical systems only, but in comprehensive aeroservoelastic systems including nonlinearities related to controllers, sensors, and actuators, the use of state form aeroelastic models must be considered a true asset. A discussion of the pros and cons of classical frequency domain and modern state-space aeroelasticity can be found in [30,31].

IV. Frequency Domain Harmonic Balance

The previously presented technique can be used to efficiently solve problems with multiple concentrated nonlinearities, including discontinuities and hystereses. From an engineering point of view, the results obtained in this way are often a well-accepted approximation for biased limit cycles. The method can be extended to two (or more) sinusoid-input DFs [8] allowing the introduction of higher harmonic contributions. However, its application is not as straightforward as for DIDF, efficiency being lost due to the complex analytic forms to be computed and to the need to combine bias terms with several harmonic contributions at the same time. A different approach is pursued here to allow a generalized numerical frequency domain harmonic balance (FDHB) with an arbitrary number of higher order harmonics. The approach is, in principle, simple and belongs to a family of methods based on functional minimization. Furthermore, it can also be applied to cases where the nonlinearity is spread and not lumped. The aeroservoelastic system can be seen as a generic nonlinear autonomous system of differential equations:

$$\boldsymbol{F}(z, \dot{z}) = \boldsymbol{0} \tag{28}$$

where the vector z represents the state variable of the system. If an autonomous limit cycle is developed, the solution must be periodic by definition, and so it can be expressed by a Fourier series characterized by an unknown circular frequency $\omega_{\rm lc}$:

$$z_{\rm lc}(t) = \sum_{i=0}^{m} \boldsymbol{b}_i \cos(i\omega_{\rm lc}t) + \sum_{i=1}^{m} \boldsymbol{c}_i \sin(i\omega_{\rm lc}t) \tag{29}$$

In this way, the constraint of periodicity is automatically satisfied, though other periodic approximation techniques can be devised. For instance, in [24], Hamilton's principle is used as the base for a periodic approximation using finite elements in time. Such a formulation sets both the LCO determination and its stability analysis à la Floquet within a single framework. It has not been pursued further here, and so an alternative solution method based on the Fourier series approximation is now explained. In such a method, the unknowns $\omega_{\rm lc}$, $\boldsymbol{b}_i$, and $\boldsymbol{c}_i$ are obtained by solving the following minimization problem of a quadratic functional [16]:

$$\min_{\omega_{\rm lc}, \boldsymbol{b}_i, \boldsymbol{c}_i} \int_0^{2\pi/\omega_{\rm lc}} \boldsymbol{\varepsilon}(t)^T\boldsymbol{\varepsilon}(t)\,{\rm d}t \tag{30}$$

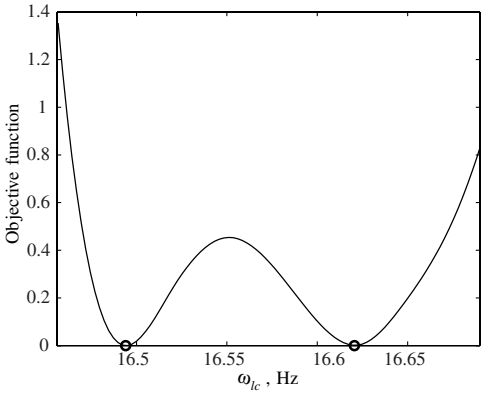

Fig. 2 Value of the quadratic functional of Eq. (30) for different assigned values of the LCO frequency ω_{lc} in the case of a double limit-cycle solution close to a turning point.

where

$$\boldsymbol{\varepsilon} = \boldsymbol{F}(z_{lc}, \dot{z}_{lc}) \tag{31}$$

To overcome possible problems related to discontinuous nonlinearities and to make the choice of the number of harmonics easier, the minimization procedure is applied in the frequency domain [17,25], because Parseval's theorem ensures the equivalence

$$\int_0^{2\pi/\omega_{lc}} \boldsymbol{\varepsilon}(t)^T \boldsymbol{\varepsilon}(t)\, \mathrm{d}t \propto \sum_{i=-\infty}^{+\infty} \boldsymbol{\varepsilon}(i\omega_{lc})^T \boldsymbol{\varepsilon}(i\omega_{lc})$$

Since $\boldsymbol{\varepsilon}$ is periodic, it can be written as

$$\boldsymbol{\varepsilon}(t) = \sum_{i=0}^{\infty} \zeta_i \cos(i\omega_{lc} t) + \sum_{i=1}^{\infty} \eta_i \sin(i\omega_{lc} t) \tag{32}$$

so that

$$\sum_{i=-\infty}^{+\infty} \boldsymbol{\varepsilon}(i\omega_{lc})^T \boldsymbol{\varepsilon}(i\omega_{lc}) = \frac{1}{2}\zeta_0^T \zeta_0 + \sum_{i=1}^{\infty} (\zeta_i^T \zeta_i + \eta_i^T \eta_i)$$

where the number of terms in the summation needs not be greater than m because of the filtering action, always present, of the linear part of the system.

The crucial aspects influencing the effectiveness of the proposed method show up in the procedure for the residual evaluation. Considering the aeroservoelastic system of Eq. (13), the residual vector is equal to

$$\boldsymbol{\varepsilon} = \boldsymbol{E}\dot{z}_{lc} - \boldsymbol{A} z_{lc} - \boldsymbol{B}_{nl} \boldsymbol{f}_{nl}(z_{lc}, \dot{z}_{lc}) \tag{33}$$

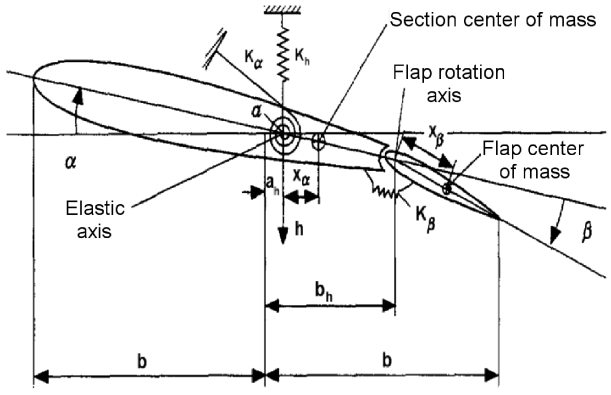

Fig. 3 Aeroelastic typical section with 3 degrees of freedom (sketch from [43]).

Table 1 Three-DOF typical section parameters

Parameter [a]	Value	Parameter	Value
b	0.724	$r_\alpha = J_\alpha/mb^2$	0.707
a_h	−0.2	$r_\beta = S_\beta/mb^2$	0.045
b_h	0.6	ω_h [b]	81.7
$x_\alpha = S_\alpha/mb$	0.0	ω_α [b]	136.0
$x_\beta = S_\beta/mb$	0.0	ω_β [b]	81.24
μ	12.0	——	——

[a]Lengths in meters.
[b]Natural uncoupled circular frequency.

Given the values for ω_{lc}, $\boldsymbol{b}_i$, and $\boldsymbol{c}_i$, the residual vector can be evaluated by using a set of sampling points distributed over the hypothetical limit-cycle period $T_{lc} = 2\pi/\omega_{lc}$. Consequently, during the optimization process, the evaluation time interval changes consistently with the evolution of the limit-cycle frequency. The sampling points have to be equally spaced to allow the use of the fast Fourier transform. This is a strong constraint that collides against the requirement of increased efficiency. In fact, when dealing with discontinuous nonlinearities, a fast sampling rate is needed close to a discontinuity crossing to guarantee an adequate accuracy. The high sampling rate used forces a growth of the evaluation cost of the residual over the LCO period and makes available a set of Fourier frequency coefficients spanning a far larger than needed frequency band. For this reason, the residual vector is low-pass filtered and decimated in the time domain before being transformed to obtain the Fourier coefficients needed for the minimization [25]. An acausal symmetric finite impulse response filter is chosen [32], its input being taken over a length of three periods T_{lc}, to enhance precision by avoiding the introduction of errors caused by both phase distortion and filter transient decay. Clearly, the calculation of the residual vector is carried out on a single period only and then reflected before and after the base time frame. The filter cutoff frequency has to be higher than the maximum frequency of interest, explained later, and, thanks to the decimation, the filtering action needs to be carried out on the retained points only. Thus, without any loss of information, we end up with a far smaller number of sampled residual vectors, which are optimally sampled for the frequency content required for a high-fidelity limit-cycle solution. Such a filtering operation also consistently smooths time domain discontinuities and helps to improve the rate of convergence of the optimization process with respect to earlier applications of the presented approach [17].

Given the ability to optimally evaluate the quadratic functional of Eq. (30), several good optimization algorithms can be employed to find a relative minimum. All the results reported in this paper have been obtained by using a procedure that is able to switch automatically between a more efficient Gauss–Newton method and a robust Levendberg–Marquadt technique [33]. Both methods require just the gradients of the objective function, which are calculated either analytically, in the time domain and then transformed, or by finite differences in the frequency domain. A mixed approach is also possible, and the choice of the calculation way is based on a matter of convenience in the treatment of the nonlinear terms at hand.

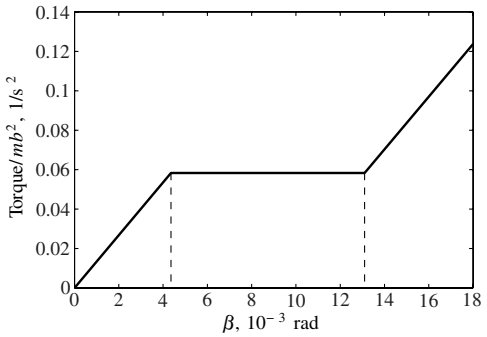

Fig. 4 Flap with a preloaded free play; torque vs flap rotation.

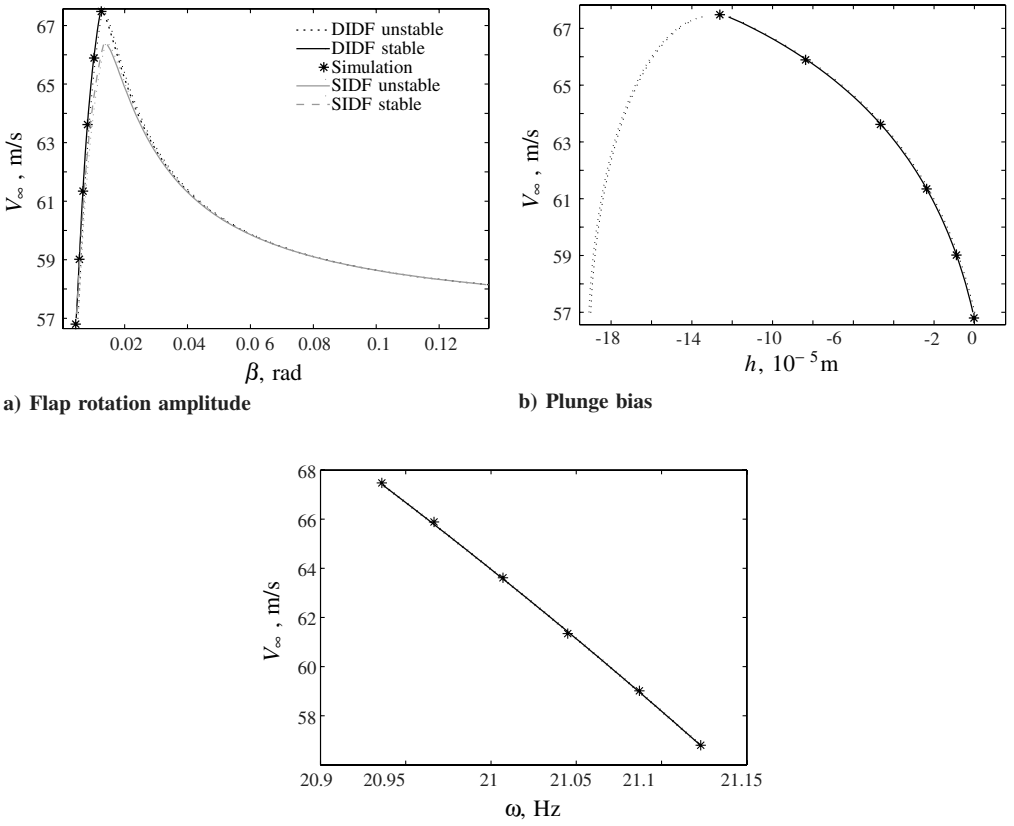

a) Flap rotation amplitude

b) Plunge bias

c) Frequency

Fig. 5 Limit cycle's results for 3-DOF typical section.

The selection of the initial tentative solution is often a serious problem, particularly for systems with many states. The main difficulty is related to the wandering of the optimizer in finding the right phase difference between the different state "signals." The availability of a first-guess solution obtained through the DIDF method presented in the previous section allows one to overcome this hurdle. In general, it might be useful to use a continued solution on the number of terms of the approximation. A kind of continuation is always needed to empirically ascertain convergence to a limit cycle by comparing a solution with m terms with one having $m + 1$.

A systematic way to avoid convergence troubles comes at the cost of parametrizing the optimization problem with respect to ω_{lc}, that is, by minimizing the functional of Eq. (30) over a set of assigned frequencies ω_{lc}. In this way, the LCO solutions are obtained by looking for stationary points (local minima) of the parametrized objective function (see Fig. 2). This approach allows one to speed up the convergence and also to verify the presence of multiple limit-cycle solutions, however close. Therefore, near limit cycle "turning points," it is possible to easily achieve a well-defined frequency convergence of the related multiple solutions. Figure 2 is related to an example to be presented later in Sec. VI.D; it shows two close stable/unstable limit cycles for which the determination greatly benefited from frequency parametrized optimization.

Table 2 Parameters for the 2-DOF typical section with hysteresis

Parameter [a]	Value	Parameter	Value
b	0.5	ω_α [b]	83.333
a_h	−0.5	ω_h [b]	100.0
$x_\alpha = S_\alpha/mb$	0.25	μ	100.0
$r_\alpha = J_\alpha/mb^2$	0.5	——	——

[a]Lengths in meters.
[b]Natural uncoupled circular frequency.

V. Limit Cycle's Stability

The study of the stability of limit cycles is a key feature to understand the behavior of the obtained solutions. Stability investigation requires the analysis of the response of the system for an exponentially shaped harmonic input, that is, $\delta e^{\sigma t}\sin(\omega t)$. Therefore, it is necessary to consider a specific DF $N(s, \delta, \gamma)$, where $s = \sigma + j\omega$ is a complex variable. In this case, Eq. (8) becomes

$$G(s)N_\delta(s, \delta, \gamma) + 1 = 0 \tag{34}$$

Once the values of δ and γ are known, the complex unknown s can be found by solving Eq. (34), thus getting an indication of the limit-cycle stability. Nonetheless, a simpler solution to the problem can be obtained through the so-called quasi-static approach. A detailed explanation of this matter can be found in [8], which reports the

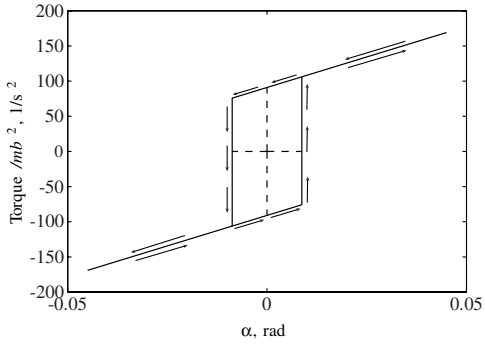

Fig. 6 Discontinuous hysteresis on the pitch degrees of freedom.

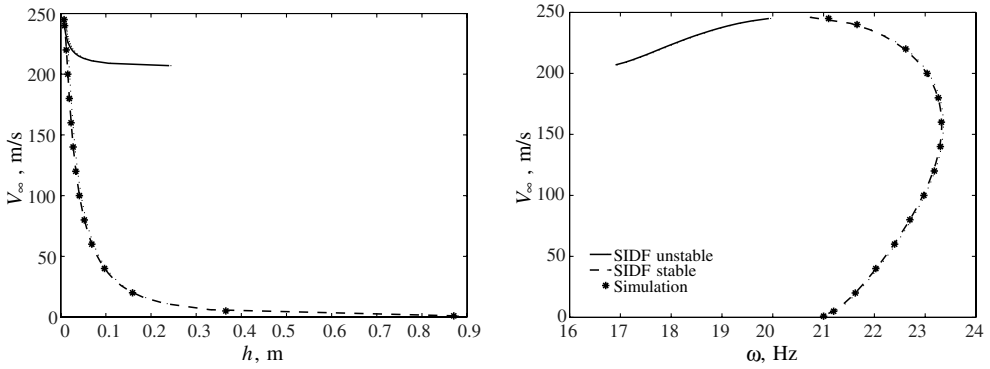

a) Plunge LCO amplitudes **b) LCO frequency**

Fig. 7 Hysteresis: limit-cycles results.

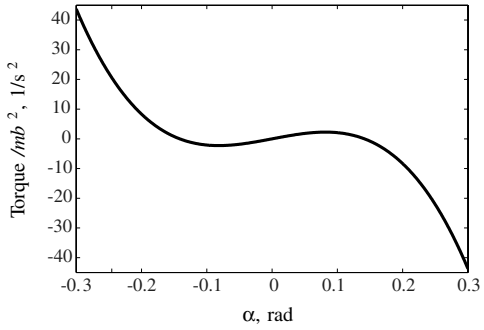

Fig. 8 Cubic restoring pitch torque: $\omega_\alpha^2 r_\alpha^2(\alpha - 50\alpha^3)$.

application to systems having only a single nonlinearity characterized by a single-input DF. Similar ideas can be found in [34,35]. Here, the same concept is extended to a generic system with multiple nonlinearities characterized by DIDFs.

The method consists in the analysis of the perturbed limit-cycle solutions to check if they tend to return onto the equilibrium periodic motion or tend to diverge from it. This is equivalent to the classical idea of static stability for linear time-invariant systems. In the case of a generic system with multiple nonlinearities, Eq. (34) can be recast in the form of homogeneous Eq. (21), which implies a null determinant for any nontrivial solution, Eq. (22), briefly indicated as

$$D(s, \alpha_{\mathrm{lc}}, \boldsymbol{\gamma}) = 0 \tag{35}$$

Through determinant differentiation, see [36], it is possible to write

$$\frac{\mathrm{d}s}{\mathrm{d}\alpha_{\mathrm{lc}}} = -\frac{\partial D(s, \alpha_{\mathrm{lc}}, \boldsymbol{\gamma})}{\partial \alpha_{\mathrm{lc}}} \Bigg/ \frac{\partial D(s, \alpha_{\mathrm{lc}}, \boldsymbol{\gamma})}{\partial s} \tag{36}$$

At the limit cycle, $s = j\omega_{\mathrm{lc}}$, and so the function can be expressed as $D(j\omega_{\mathrm{lc}}, \alpha_{\mathrm{lc}}, \boldsymbol{\gamma})$. Assuming $D \in \mathbb{C}$ is an analytic function, the derivatives of Eq. (36) can be expanded in the following way:

$$\frac{\partial D(s, \alpha_{\mathrm{lc}}, \boldsymbol{\gamma})}{\partial \alpha_{\mathrm{lc}}} = \frac{\partial \Re[D]}{\partial \alpha_{\mathrm{lc}}} + j\frac{\partial \Im[D]}{\partial \alpha_{\mathrm{lc}}} \tag{37}$$

$$\frac{\partial D(s, \alpha_{\mathrm{lc}}, \boldsymbol{\gamma})}{\partial s} = \frac{\partial D(s, \alpha_{\mathrm{lc}}, \boldsymbol{\gamma})}{\partial j\omega} = -j\frac{\partial \Re[D]}{\partial \omega} + \frac{\partial \Im[D]}{\partial \omega} \tag{38}$$

Using Eqs. (36–38), the explicit derivatives of the real and the imaginary parts of s become

$$\frac{\mathrm{d}\sigma}{\mathrm{d}\alpha_{\mathrm{lc}}} = \frac{\frac{\partial \Re[D]}{\partial \omega}\frac{\partial \Im[D]}{\partial \alpha_{\mathrm{lc}}} - \frac{\partial \Re[D]}{\partial \alpha_{\mathrm{lc}}}\frac{\partial \Im[D]}{\partial \omega}}{(\frac{\partial \Re[D]}{\partial \omega})^2 + (\frac{\partial \Im[D]}{\partial \omega})^2} \tag{39}$$

$$\frac{\mathrm{d}\omega}{\mathrm{d}\alpha_{\mathrm{lc}}} = -\frac{\frac{\partial \Im[D]}{\partial \alpha_{\mathrm{lc}}}\frac{\partial \Im[D]}{\partial \omega} + \frac{\partial \Re[D]}{\partial \alpha_{\mathrm{lc}}}\frac{\partial \Re[D]}{\partial \omega}}{(\frac{\partial \Re[D]}{\partial \omega})^2 + (\frac{\partial \Im[D]}{\partial \omega})^2} \tag{40}$$

Now, according to our criteria, the stability of the LCO is satisfied when $\mathrm{d}\sigma/\mathrm{d}\alpha_{\mathrm{lc}} < 0$, which is summarized by the following requirement:

$$\frac{\partial \Re[D]}{\partial \omega}\frac{\partial \Im[D]}{\partial \alpha_{\mathrm{lc}}} - \frac{\partial \Re[D]}{\partial \alpha_{\mathrm{lc}}}\frac{\partial \Im[D]}{\partial \omega} < 0 \tag{41}$$

The computation of the determinant D and its derivatives can be extremely cumbersome, so that it is more efficient and straightforward to proceed by determining $\mathrm{d}\sigma/\mathrm{d}\alpha_{\mathrm{lc}}$ directly from Eq. (25). Once more, thanks to having cast an eigenvalue-like problem into a nonlinear system of equations, the computation of such a derivative is conceptually trivial, being tantamount to rewriting Eq. (26) with σ as a new unknown in place of α_{lc}, whereas the latter takes the place of a parameter p [21]. In such a view $\mathrm{d}\sigma/\mathrm{d}\alpha_{\mathrm{lc}}$ is the derivative of the solution of Eq. (25), with ω_{lc} substituted by $s_{\mathrm{lc}} = 0 + j\omega_{\mathrm{lc}}$. This approach unifies the simplified DIDF approximation to a well-tested and reliable solution framework used for linear flutter analyses, which has found large usage both in large parametrized analyses and

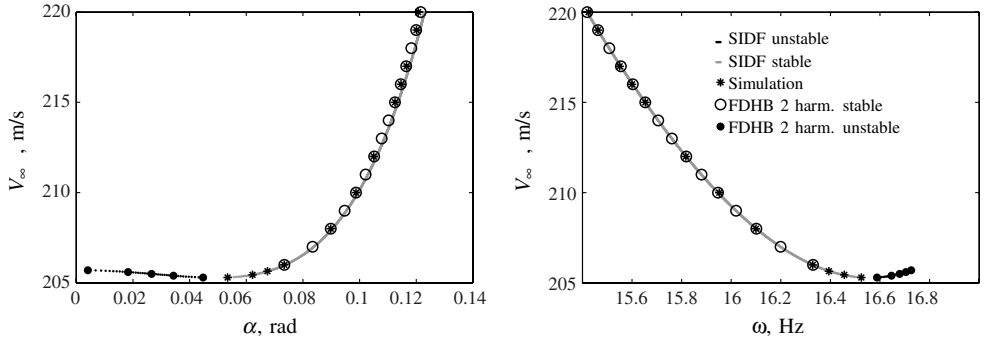

a) Pitch LCO amplitudes **b) LCO frequency**

Fig. 9 Softening: limit-cycles results.

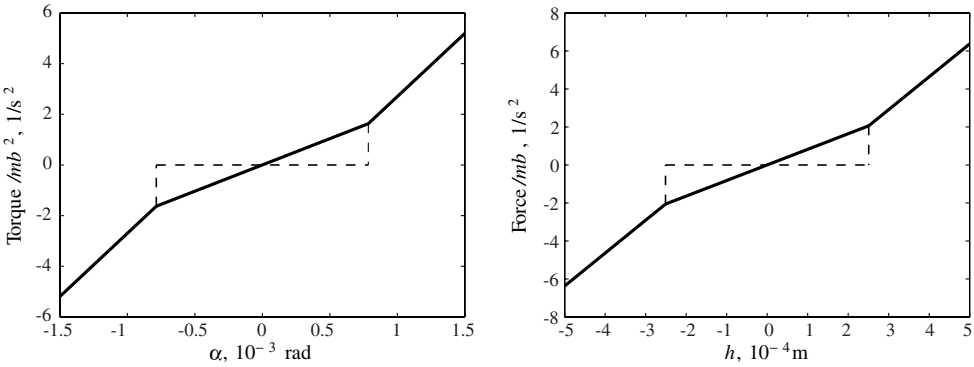

a) Pitch b) Plunge

Fig. 10 Bilinear nonlinearities.

in setting up flutter constraints in automated and integrated optimization methods [37–40].

For a multiple harmonics solution obtained through the functional minimization approach, the Floquet method should be used to assess stability [1,41,42]. Consider a nonlinear autonomous implicit system of differential equations

$$\boldsymbol{F}(z, \dot{z}) = \boldsymbol{0} \tag{42}$$

showing a periodic limit-cycle solution $z_{\mathrm{lc}}(t)$ having period $2\pi/\omega_{\mathrm{lc}}$. Equation (42) can be linearized around $z_{\mathrm{lc}}(t)$, thus writing

$$\boldsymbol{0} = \boldsymbol{F}|_{z=z_{\mathrm{lc}}} + \left.\frac{\partial \boldsymbol{F}}{\partial z}\right|_{z=z_{\mathrm{lc}}} \delta z + \left.\frac{\partial \boldsymbol{F}}{\partial \dot{z}}\right|_{z=z_{\mathrm{lc}}} \delta \dot{z} \tag{43}$$

Knowing that $\boldsymbol{F}|_{z=z_{\mathrm{lc}}} = \boldsymbol{0}$, the following first-order periodic linear system results

$$\frac{\partial \boldsymbol{F}}{\partial \dot{z}} \delta \dot{z} + \frac{\partial \boldsymbol{F}}{\partial z} \partial z = \boldsymbol{0} \tag{44}$$

And so, the stability of the motion $z_{\mathrm{lc}}(t)$ can be investigated by introducing the transition matrix $\boldsymbol{Q}(t)$

$$\frac{\partial \boldsymbol{F}}{\partial \dot{z}} \dot{\boldsymbol{Q}}(t) + \frac{\partial \boldsymbol{F}}{\partial z} \boldsymbol{Q}(t) = \boldsymbol{0} \tag{45}$$

and the knowledge of the eigenvalues of the monodromy matrix $\boldsymbol{Q}(T_{\mathrm{lc}})$. To obtain $\boldsymbol{Q}(T_{\mathrm{lc}})$, Eq. (45) is integrated n times on the interval $(0, T_{\mathrm{lc}})$ with the n initial conditions $\boldsymbol{Q}(0) = \boldsymbol{I}$.

A limit cycle is stable if all the eigenvalues of the monodromy matrix but one have a norm lower than one.[§] If at least one eigenvalue has a module higher than one, the solution is unstable, whereas, in the presence of more than one unit, eigenvalues system stability will be related to the Jordan form associated to the transition matrix.

VI. Numerical Results

The two numerical methods presented are now applied to figure out the characteristics of LCOs for several aeroelastic models with lumped nonlinearities. All the problems have been solved following a standard procedure. First, possible LCOs have been determined using the DIDF method. Then, the functional minimization based on FDHB has been used to check for possible improvements by adding higher harmonics. The two methods described in Sec. V have been exploited to evaluate the stability of the identified LCOs. Finally, the results have been compared to solutions obtained through direct numerical integration, which can reproduce only stable LCOs. This property has been used to indirectly verify the correctness of the stability evaluation.

[§]There is always one eigenvalue associated with perturbations along the limit cycle in the phase space that is equal to one.

A. Three-Degrees-of-Freedom Aeroelastic Typical Section with Free Play

This model represents a 3-degrees-of-freedom typical aeroelastic section [26,43], with a preloaded free-play nonlinearity on the flap stiffness. The unsteady aerodynamic forces have been described using Theodorsen's model [44,45] transformed into a linear time-invariant state-space form through a second-order approximation. The aeroelastic system shown in Fig. 3 is characterized by eight states, and its main parameters are summarized in Table 1. Figure 4 shows the nonlinearity in the flap hinge.

The preload causes an asymmetric LCO. Figures 5a and 5b show, respectively, the limit-cycle amplitudes for the first harmonic of flap rotation β and the plunge bias component for different flight velocities. Figure 5a shows the excellent agreement between the direct integration and the DIDF results, whereas some tests carried out with the single-input describing function (SIDF) reveal inaccuracies, especially close to the turning point. The application of the FDHB to this problem does not improve the limit-cycle solutions found using the DIDF, thus proving the low-pass filtering property of the linear part of the system. Stability analyses comply with the results of direct integrations.

B. Two-Degrees-of-Freedom Typical Section with Hysteresis

This problem considers a simpler typical section with only 2 degrees of freedom [27,46], that is, without flap, with aerodynamics modeled as for the previous example. A nonlinearity with hysteresis and discontinuity has been put on the pitch rotation. The problem data are summarized in Table 2, and Fig. 6 shows the lumped nonlinearity. The presence of a hysteresis requires a complex describing function, that is, one with quasi-linear stiffness and a quasi-linear damping contribution. Figures 7a and 7b show the frequency of the LCO and the amplitude of the plunge at different velocities. Here, the symmetric nonlinearity allows one to use the SIDF, the FDHB providing no further improvement. The comparison with the direct integration proves the ability of the describing function method in finding the correct solutions with accuracy and efficiency. The good correlation between direct integration results and the SIDF method demonstrate the negligible contributions of higher harmonics. The stability evaluation is again confirmed by direct simulation.

Table 3 Parameters for the 2-DOF typical section with bilinear stiffness

Parameter [a]	Value	Parameter	Value
b	0.1257	ω_{1h} [b]	90.61
a_h	−0.297	ω_{2h} [b]	112.9
$x_\alpha = S_\alpha/mb$	0.0196	$\omega_{1\alpha}$ [b]	89.32
$r_\alpha = J_\alpha/mb^2$	0.51	$\omega_{2\alpha}$ [b]	115.39
μ	95.81	——	——

[a]Lengths in meters.
[b]Natural uncoupled circular frequency.

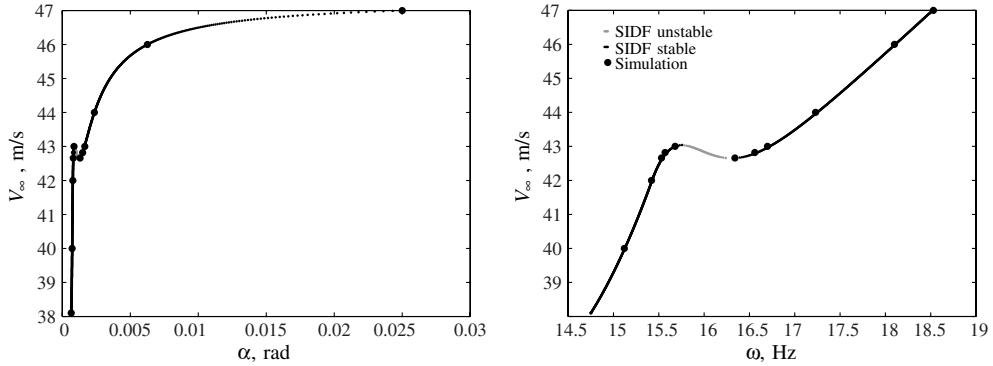

a) Pitch LCO amplitudes **b) LCO frequency**

Fig. 11 Bilinear stiffness: limit-cycles results.

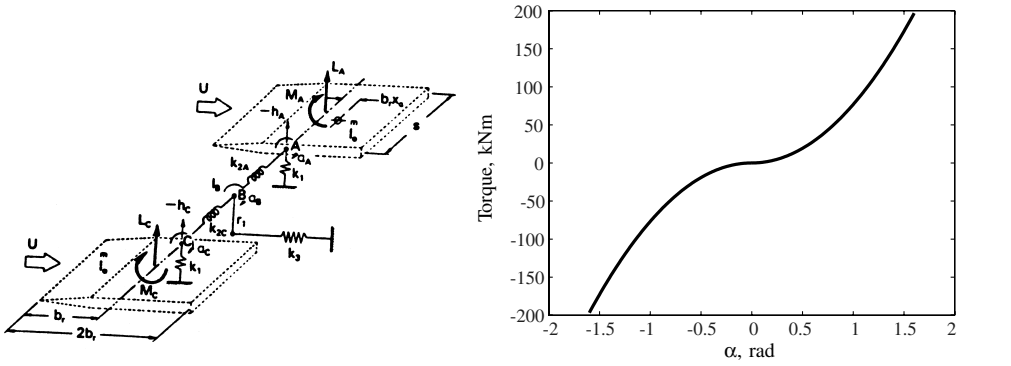

a) Tail model sketch from [9] **b) Parabolin nonlinearity:** $M_{\alpha_A} = K_{2A}(\alpha_A - \alpha_B)\|\alpha_A - \alpha_B\|$

Fig. 12 Characteristics of nonlinear tail model in supersonic regime.

C. Two-Degrees-of-Freedom Typical Section with Cubic Stiffness

This example reworks the previous 2-degrees-of-freedom typical section with a softening cubic stiffness on the pitch restoring torque (see Table 2). The nonlinearity is pictured in Fig. 8. Figures 9a and 9b, respectively, show the LCO pitch amplitude and the LCO frequency at different flight velocities. Both figures present a turning point where there is a frequency convergence of the stable and unstable solutions. In fact, the related close frequencies are those presented during the explanation of the frequency parametrized FDHB, that is, Fig. 2. At high velocities, it is possible to see the loss of accuracy of the stable pitch limit cycle computed by DIDF vis-à-vis to a two harmonics FDHB, Fig. 9. Solutions up to four harmonics have been computed using FDHB showing no appreciable differences. The limit-cycles stability study is in accordance with numerical integration evidences.

D. Two-Degrees-of-Freedom Typical Section with Bilinear Stiffness

In this case, the 2-degrees-of-freedom typical section is analyzed with two bilinear nonlinearities on the pitch and plunge degrees of freedom. Figures 10a and 10b show the two nonlinearities, and the model parameters are summarized in Table 3. Figure 11a shows the pitch limit-cycle amplitudes with the presence of a double turning point, which is quite typical for problems with multiple nonlinearities. In Fig. 11b, it is possible to appreciate the limit-cycle frequency corresponding to different velocities. In this case, the nonlinearity is symmetric, and so SIDFs have been used. FDHB easily solves this model showing, once more, that higher harmonic contributions to limit cycles are negligible. Limit-cycles stability evaluations agree with numerical integrations again.

Table 4 Parameters for the airplane tail in supersonic regime

Parameter	Value	Unit	Parameter	Value	Unit
m	4.545	kg	r_1	0.0762	m
b_r	0.254	m	s	0.254	m
x_0	0.2	——	J_0	0.2984	kgm^2
K_1	70.04	kN/m	J_B	0.0594	kgm^2
K_{2A}	76.8159	kNm/rad	Mach	2.0	——
K_{2C}	76.8159	kNm/rad	ρ	0.5957	kg/m^3
K_3	4377.3	kN/m	——	——	——

E. Airplane Tail in Supersonic Regime

As final example, we propose a 5-degrees-of-freedom airplane tail in supersonic regime already proposed in [9]. The tail is sketched in Fig. 12a. Two equal parabolic nonlinearities are placed on the flaps' pitch, as shown in Fig. 12b. The supersonic aerodynamics are described using the zero-order piston theory [26], thus leading to a 10 states model. All model data are summarized in Table 4. Figures 13a and 13b represent, respectively, the pitch and plunge flap limit-cycle amplitudes, whereas Fig. 13c shows the LCOs frequencies. The solution for the two flaps is symmetric with a phase difference of 180 deg, and so the central node, which represents the fuselage rotation degree of freedom, maintains a null value. The SIDF method can approximate the solution, but Fig. 13a shows a loss of accuracy at high velocity values. The FDHB does show improvements in the solution accuracy by using at least two harmonics. Figures 13a and 13b show the excellent correlation of the results of FDHB with numerical integration even for high velocity values. Figures 14b and 14a highlight the level of accuracy on the limit-cycle trajectory of the different methods. The stability study gives the usual correct answer in accordance with direct integration results.

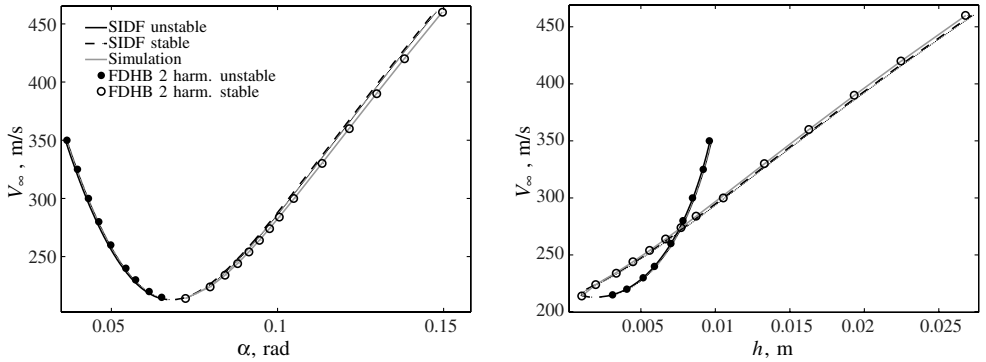

a) LCO pitch amplitudes

b) LCO plunge amplitude

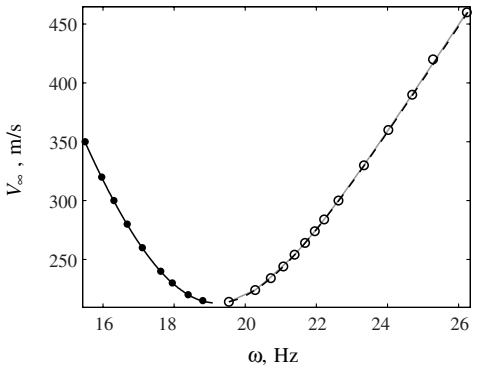

c) LCO frequency

Fig. 13 Limit-cycles results for tail model; the two flaps are out of phase by 180 deg.

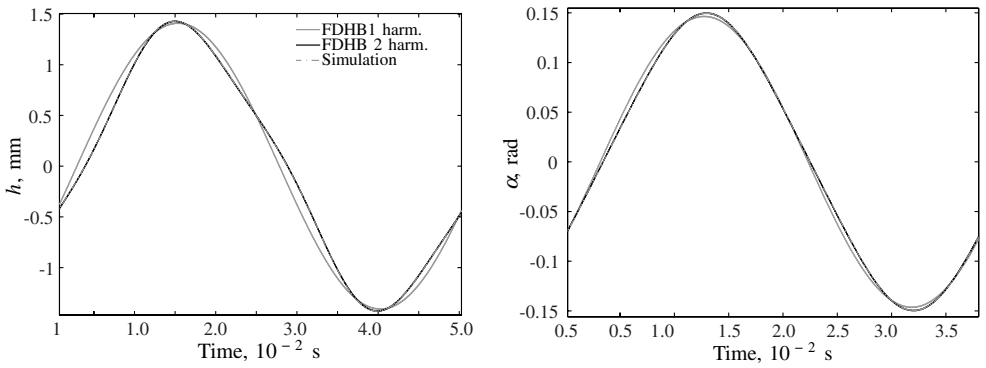

a) Plunge at 220 m/s

b) Pitch at 460 m/s

Fig. 14 Comparison of LCO trajectories for different approximation level.

VII. Conclusions

The methods presented have demonstrated their ability to compute limit cycles of multi-degrees-of-freedom systems with multiple lumped nonlinearities. The formulation based on describing functions comes as a natural extension of the direct calculation of the linear flutter condition. It often leads to very good approximations, thanks to the low-pass filtering action shown by the linear part of aeroelastic systems. The adoption of dual-input describing functions allows one to solve asymmetric as well as symmetric limit cycles. Therefore, a wide variety of nonlinear terms, including discontinuous functions and hysteresis, can be easily handled. For systems which do not show a sufficient low-pass filtering action, the method based on functional minimization in the frequency domain can improve the solution accuracy by adding the needed higher harmonics. The overall approach has demonstrated its capability to handle different kind of nonlinearities. The additional procedures introduced for the investigation of the stability of limit cycles have shown their soundness and efficiency against the results obtained through direct numerical integration.

References

[1] Sastry, S., "Nonlinear Systems: Analysis, Stability and Control," *Interdisciplinary Applied Mathematics*, Vol. 10, Springer–Verlag, New York, 1999.

[2] Woolstone, D., Runyan, H., and Andrews, R., "An Investigation of Effects of Certain Type of Structural Nonlinearities on Wing and Control Surface Flutter," *Journal of the Aeronautical Sciences*, Vol. 24, No. 1, 1957, pp. 57–63.

[3] Shen, S., "An Approximate Analysis of Nonlinear Flutter Problems," *Journal of the Aerospace Sciences*, Vol. 26, No. 1, 1959, pp. 25–31.

[4] Thomas, J., Dowell, E., and Hall, K., "Nonlinear Inviscid Aerodynamic Effects on Transonic Divergence, Flutter, and Limit-Cycle Oscillations," *AIAA Journal*, Vol. 40, No. 4, April 2002, pp. 638–646.
doi:10.2514/2.1720

[5] Breitbach, E., "Effect of Structural Nonlinearities on Aircraft Vibration and Flutter," AGARD, TR 665, Jan. 1977.
[6] Lee, B., Price, S., and Wong, Y., "Nonlinear Aeroelastic Analysis of Airfoils: Bifurcation and Chaos," *Progress in Aerospace Sciences*, Vol. 35, No. 3, 1999, pp. 205–334. doi:10.1016/S0376-0421(98)00015-3
[7] Dowell, E. H., Edwards, J., and Strganac, T., "Nonlinear Aeroelasticity," *Journal of Aircraft*, Vol. 40, No. 5, 2003, pp. 857–874. doi:10.2514/2.6876
[8] Gelb, A., and Vander Velde, W. E., *Multiple-Input Describing Functions and Nonlinear System Design*, McGraw–Hill, New York, 1968.
[9] Lee, C. L., "An Iterative Procedure for Nonlinear Flutter Analysis," *AIAA Journal*, Vol. 24, No. 5, 1986, pp. 833–840. doi:10.2514/3.9352
[10] Zhao, L. C., and Yang, Z. C., "Chaotic Motions of an Airfoil with Non-Linear Stiffness in Incompressible Flow," *Journal of Sound and Vibration*, Vol. 138, No. 2, 1990, pp. 245–254. doi:10.1016/0022-460X(90)90541-7
[11] Tang, D., Dowell, E. H., and Virgin, L. N., "Limit Cycle Behavior of an Airfoil with a Control Surface," *Journal of Fluids and Structures*, Vol. 12, No. 7, 1998, pp. 839–858. doi:10.1006/jfls.1998.0174
[12] Liu, L., and Dowell, E. H., "The Secondary Bifurcation of an Aeroelastic Airfoil Motion: Effect of High Harmonics," *Nonlinear Dynamics*, Vol. 37, No. 1, 2004, pp. 31–39. doi:10.1023/B:NODY.0000040033.85421.4d
[13] Gordon, J., Meyer, E., and Minogue, R., "Nonlinear Stability Analysis of Control Surface Flutter with Free-Play Effects," *Journal of Aircraft*, Vol. 45, No. 6, 2008, pp. 1904–1916. doi:10.2514/1.31901
[14] Vio, G., Dimitriadis, G., and Cooper, J., "Bifurcation Analysis and Limit Cycle Oscillation Amplitude Prediction Methods Applied to the Aeroelastic Galloping Problem," *Journal of Fluids and Structures*, Vol. 23, No. 7, 2007, pp. 983–1011. doi:10.1016/j.jfluidstructs.2007.03.006
[15] Liu, L., Thomas, J. P., Dowell, E. H., Attar, P., and Hall, K. C., "A Comparison of Classical and High Dimensional Harmonic Balance Approaches for a Duffing Oscillator," *Journal of Computational Physics*, Vol. 215, No. 1, June 2006, pp. 298–320. doi:10.1016/j.jcp.2005.10.026
[16] Cocetta, S., "Oscillazioni Nonlineari e Cicli Limite: un Approccio Numerico per Collocazione ai Minimi Quadrati, M.S. Thesis, Dept. di Ingegneria Aerospaziale, Politecnico di Milano, Milan, 1987.
[17] Bertola, E., "Oscillazioni Nonlineari e Cicli Limite Mediante Collocazione ai Minimi Quadrati nel Dominio delle Frequenze," M.S. Thesis, Dept. di Ingegneria Aerospaziale, Politecnico di Milano, Milan, 1989.
[18] Taylor, J., *Wiley Encyclopedia of Electrical and Electronics Engineering*, Chap. Describing Functions, Wiley, New York, 1999, pp. 77–98.
[19] Krylov, N., and Bogolyubov, N., *Introduction to Nonlinear Mechanics*, Princeton Univ. Press, Princeton, NJ, 1947.
[20] Cardani, C., and Mantegazza, P., "Continuation and Direct Solution of the Flutter Equation," *Computers & Structures*, Vol. 8, No. 2, 1976, pp. 185–192.
[21] Cardani, C., and Mantegazza, P., "Calculation of Eigenvalue and Eigenvector Derivatives for Algebraic Flutter and Divergence Eigenproblems," *AIAA Journal*, Vol. 17, No. 4, 1979, pp. 408–412. doi:10.2514/3.61140
[22] Giavotto, V., Mantegazza, P., Otto, L. D., Lucchesini, M., and Mantelli, R., "Fast Flutter Clearance by Parameter Variation," AGARD, CP 354, Sept. 1983.
[23] Seydel, R., *Practical Bifurcation and Stability Analysis: From Equilibrium to Chaos*, Springer–Verlag, New York, 1994.
[24] Borri, M., and Mantegazza, P., "Nonlinear Oscillation and Limit Cycles: A Numerical Approach by Finite Elements in Time Domain," *Sixth International Conference on Mathematical Modelling*, Aug. 1987.
[25] Manetti, M., "Metodi Numerici per lo Studio di Cicli Limite Applicati a Sistemi Aeroelastici," M.S. Thesis, Dept. di Ingegneria Aerospaziale, Politecnico di Milano, Milan, 2005.
[26] Bisplinghff, R. L., and Ashley, H., *Principles of Aeroelasticity*, Wiley, New York, 1962.
[27] Price, S., Alinghanbari, H., and Lee, B., "The Aeroelastic Response of a Two-Dimensional Airfoil with Bilinear and Cubic Structural Nonlinearities," *Journal of Fluids and Structures*, Vol. 9, No. 2, 1995, pp. 175–193. doi:10.1006/jfls.1995.1009
[28] Pasinetti, G., and Mantegazza, P., "Single Finite States Modeling of Aerodynamic Forces Related to Structural Motions and Gusts," *AIAA Journal*, Vol. 37, No. 5, May 1999, pp. 604–612. doi:10.2514/2.760
[29] Ortega, J., and Rheinboldt, W., "Iterative Solution of Nonlinear Equations in Several Variables," *Classics in Applied Mathematics*, Vol. 20, Society for Industrial and Applied Mathematics, Philadelphia, 2000.
[30] Lanz, M., and Mantegazza, P., "Numerical Methods for Predicting the Aeroelastic Stability and Response of Flexible Airplanes," *L'Aerotecnica, Missili e Spazio*, Vol. 63, No. 2, 1984, pp. 105–118.
[31] Lanz, M., and Mantegazza, P., "Modern Methods for the Analysis of the Dynamic Response of Aeroelastic Systems," *L'Aerotecnica, Missili e Spazio*, Vol. 64, No. 3, 1985, pp. 170–176.
[32] Oppenheim, A., Schafer, R., and Buck, J., *Discrete-Time Signal Processing*, Prentice–Hall, Upper Saddle River, NJ, 1999.
[33] Kelley, C., "Iterative Methods for Optimization," *Frontiers in Applied Mathematics*, Vol. 18, Society for Industrial and Applied Mathematics, Philadelphia, 1999.
[34] Somieski, G., "An Eigenvalue Method for Calculation of Stability and Limit Cycles in Nonlinear Systems," *Nonlinear Dynamics*, Vol. 26, No. 1, 2001, pp. 3–22. doi:10.1023/A:1017384211491
[35] Stojic, M., and Siljak, D., "Sensitivity Analysis of Self-Excited Oscillations in Nonlinear Control Systems," *Proceedings to Sensitivity Methods in Control Theory*, edited by L. Radnovic, Pergamon, Oxford, England, U.K., 1964, pp. 209–219.
[36] Golberg, M., "The Derivative of a Determinant," *The American Mathematical Monthly*, Vol. 79, No. 10, 1972, pp. 1124–1126. doi:10.2307/2317435
[37] Bindolino, G., Mantegazza, P., and Ricci, S., "Integrated Servostructural Optimization in the Design of Aerospace Systems," *Journal of Aircraft*, Vol. 36, No. 1, 1999, pp. 167–175. doi:10.2514/2.2423
[38] Bindolino, G., Ghiringhelli, G., and Ricci, S., "Preliminary Sizing of the Wing-Box Structure by Multi-Level Approach," Confederation of European Aerospace Societies/Deutsche Gesellschaft fr Luft- und Raumfarht/AIAA Paper IF-001, 2005.
[39] Cavagna, L., Riccobene, L., Ricci, S., Berard, A., and Rizzi, A., "Fast MDO Tool for Aeroelastic Optimization in Aircraft Conceptual Design," AIAA Paper 2008-5911, 2008.
[40] Ghiringhelli, G., and Ricci, S., "A Multi-Level Approach to Preliminary Optimization of a Wing Structure," Vol. 1, Associacion de Ingenieros Aeronauticos de Espana, Madrid, 2001.
[41] Sansone, G., and Conti, R., *Non-linear Differential Equations*, Translated from Italian by A. H. Diamond, Pergamon Press, Oxford, England, U.K., 1964.
[42] Burton, T. A., *Stability and Periodic Solutions of Ordinary and Functional Differential Equations*, Academic Press, Orlando, FL, 1985.
[43] Virgin, L., Dowell, E., and Conner, M., "On the Evolution of Deterministic Non-Periodic Behavior of an Airfoil," *International Journal of Non-Linear Mechanics*, Vol. 34, No. 3, 1998, pp. 499–514. doi:10.1016/S0020-7462(98)00038-9
[44] Theodorsen, T., "General Theory of Aerodynamic Instability and the Mechanism of Flutter," NACA, TR 496, 1935.
[45] Bisplinghoff, R. L., Ashley, H., and Halfman, R. L., *Aeroelasticity*, Addison Wesley, New York, 1955.
[46] Lee, B., Gong, L., and Wong, Y., "Analysis and Computation of Nonlinear Dynamic Response of a Two-Degree-of-Freedom System and its Application in Aeroelasticity," *Journal of Fluids and Structures*, Vol. 11, No. 3, 1997, pp. 225–246. doi:10.1006/jfls.1996.0075